Spatial Assessment of Urban Flood Vulnerability in Polk County, Iowa Using a Social–Ecological–Technological Framework

Ege Duran†[1,2*], Atiye Beyza Cikmaz†[1], Jerry Mount [1], Ibrahim Demir [3,4]

[1] IIHR, Hydroscience and Engineering, University of Iowa, Iowa City, IA, USA
[2] Civil and Environmental Engineering, University of Iowa, Iowa City, IA, USA
[3] River-Coastal Science and Engineering, Tulane University, New Orleans, LA, USA
[4] ByWater Institute, Tulane University, New Orleans, LA, USA

† These authors contributed equally to this work.
*Corresponding Author: Ege Duran, ege-duran@uiowa.edu

Abstract

Flood impacts are shaped not only by environmental or economic consequences but also by the social, ecological, and infrastructural conditions that influence how communities experience and recover from hazards. This study aims to assess multi-domain flood vulnerability across Polk County, Iowa utilizing a Social–Ecological–Technological Systems (SETS) framework. Eighteen indicators were standardized and aggregated to produce domain-specific and composite indices, which were evaluated independently from mapped flood exposure at the census block group scale. Results show that social, ecological, and technological vulnerabilities exhibit distinct and non-coincident spatial patterns, while composite indices reveal broader zones where multiple weaknesses co-occur. The highest compounded susceptibility is concentrated in the Des Moines urban core and along the Des Moines River corridor, although each domain highlights different localized patterns across the county. Weak correlations between vulnerability scores and flood extent support that intrinsic susceptibility and hydraulic exposure represent separate and complementary processes. Overall, the framework provides a transparent and transferable approach to support targeted mitigation, planning, and resilience strategies in flood-prone urban communities.

Keywords: SET systems, Flood Vulnerability, Disaster Risk Assessment, Urban Flood, Exposure

1. Introduction

Floods are among the most destructive natural hazards worldwide, causing substantial loss of life, economic damage, and long-term disruption to communities and infrastructure (Saharia et al., 2017; Alabbad & Demir, 2024). Their frequency and severity have increased in recent decades due to intensifying precipitation extremes, land-use change, and expanding urbanization (Huang et al., 2022; Sadler et al., 2017; Li et al., 2023a). Unlike many hazards, floods can develop rapidly and persist for days or even weeks depending on terrain, drainage capacity, and storm duration, which complicates emergency response and prolongs recovery efforts (Lebbe et al., 2014; Duran et al., 2025a). In the United States, floods remain one of the most costly and recurrent disasters, affecting millions of residents and critical services each year (Retchless et al., 2014; Zhou et al., 2018). Especially, the Midwest region experiences particularly elevated flood risk because of seasonal heavy rainfall, extensive river systems, and low-gradient landscapes that promote widespread inundation (Dirmeyer and Kinter III, 2010). These conditions create persistent exposure of populations, ecosystems, and infrastructure, and highlight the need for systematic approaches to evaluate and manage flood impacts.

To address these escalating risks, the evolution of modern flood risk management is increasingly defined by the synergy between traditional geoscience and emerging data science methodologies, necessitating robust frameworks for benchmarking interdisciplinary efforts (Ebert-Uphoff et al., 2017). Recent research highlights this transition through the comparison of artificial intelligence and traditional hydrologic insights for real-time streamflow forecasting, underscoring the need for high-fidelity predictive tools (Krajewski et al., 2021). Furthermore, the scope of hydrological monitoring has been significantly expanded by the rise of crowdsourced data collection via smartphones and the utilization of distributed volunteer computing for large-scale research applications (Sermet et al., 2020; Agliamzanov et al., 2020). These technological advancements are further complemented by web-based geovisual analytics that allow for the identification of localized infrastructural vulnerabilities, such as those impacting culvert sedimentation (Xu et al., 2019). While these tools improve our understanding of hydraulic exposure and data accessibility, a holistic assessment of flood risk requires understanding the intrinsic vulnerabilities that determine how communities experience and recover from hazards.

Within this framework, Iowa serves as a critical case study as it exhibits persistent susceptibility to flooding due to its unique physiographic setting and history of recurrent high-magnitude events. The state is shaped by major river systems, including the Mississippi River to the east and the Missouri River to the west, which create broad floodplains and extensive inundation pathways (Li et al., 2023b). Historical records document repeated large-scale floods that have disrupted communities, infrastructure, and agricultural production, most notably the 2008 event, which ranks among the costliest disasters in the state and caused widespread damage to homes, transportation networks, and public facilities (USGS, 2010; Zogg, 2014). More recent floods have continued to affect multiple regions of Iowa, producing substantial economic losses and demonstrating that exposure remains spatially widespread rather than isolated (Alabbad & Demir, 2025). Flooding in Iowa is therefore not episodic but systemic. It repeatedly affects

population centers, critical infrastructure, and essential services, which underscores the need to assess local vulnerability conditions alongside hazard mapping.

Flood vulnerability assessment has increasingly shifted from hazard-only mapping toward approaches that explicitly consider exposure, sensitivity, and adaptive capacity to better represent how communities and infrastructure experience flood impacts (Nasiri, 2016; De Brito et al., 2018). Indicator-based methods have become common because they integrate social, environmental, and physical factors and enable spatial comparison of susceptibility across locations (Nguyen et al., 2023). However, these assessments often differ in indicator selection, domain coverage, and aggregation strategies, which can limit consistency and transferability across study areas. Although integrated frameworks such as the social–ecological–technological (SETS) structure have been proposed to address this fragmentation (Chang et al., 2021), comprehensive applications that jointly evaluate multiple domains within a unified concept remain limited. In Iowa, repeated flood events have prompted numerous advanced assessments of risk, exposure, and community-scale impacts, including case studies evaluating flood effects on the built environment and local vulnerability patterns (Duran et al., 2025b; Alabbad et al., 2024). Despite these advances, a standardized and transparent framework that jointly characterizes social, ecological, and technological conditions remains limited. Such integration is necessary to represent intrinsic susceptibility independently from hazard exposure and to enable consistent comparisons across space (Chang et al., 2021; Sauer et al., 2023).

Conceptualizing communities as interconnected social–ecological systems has become common in resilience and risk research, with applications spanning coastal zones, forest governance, marine management, and fisheries (Cinner et al., 2013; Rives et al., 2012; Lauerburg et al., 2020; Lazzari et al., 2021). Yet flood-related assessments frequently emphasize social and environmental characteristics (Cikmaz et al., 2023), and threat technological and infrastructure elements as secondary or external components. Only a limited set of studies explicitly integrate social, ecological, and technological dimensions within a unified framework, and these applications typically address ecosystem services or urban transformation rather than comprehensive flood vulnerability (Bixler et al., 2019; McPhearson, 2022; Sauer, 2023). Building on the holistic SETS structure articulated by Chang et al. (2021), this study adopts an integrated, tri-domain approach that systematically incorporates all three components to evaluate compounded flood susceptibility within a single, consistent framework.

To address these gaps, this study implements a Social–Ecological–Technological Systems (SETS) framework to develop both domain-specific and composite flood vulnerability indices and evaluates their relationship with independently observed flood exposure. The analysis is conducted at the census block group scale for Polk County, Iowa, which contains the state's largest population center and concentrated infrastructure, making it a representative setting for examining how compounded social, environmental, and technological susceptibilities translate into real-world flood impacts (Duran et al., 2025c). By separating intrinsic vulnerability from the flood footprint and integrating multiple domains within a consistent structure, the proposed approach provides a

transparent and transferable framework that supports spatial comparison, prioritization of mitigation actions, and informed decision-making rather than producing isolated score sets.

The remainder of this paper is organized as follows. Section 2 describes the methodology, including the case study characteristics, the Social–Ecological–Technological Systems (SETS) framework, data preparation procedures, vulnerability index computation, and statistical evaluation methods. Section 3 presents the results and discussion, beginning with domain-specific vulnerability patterns, followed by composite indices and statistical and spatial evaluations. Finally, Section 4 summarizes the main findings, implications, limitations, and directions for future research.

2. Methodology

This section outlines the methodological framework used to assess flood vulnerability across Polk County using the Social–Ecological–Technological Systems (SETS) approach. The workflow includes defining the study area and hazard context, selecting and preparing social, ecological, and technological indicators, normalizing variables and constructing domain-specific and composite vulnerability indices, and conducting statistical analyses to evaluate relationships with flood exposure and the stability of the resulting scores. These steps establish a systematic and reproducible procedure for quantifying spatial patterns of susceptibility and identifying locations where underlying conditions intensify flood impacts.

2.1. Case Study Area

This study was conducted in Polk County, Iowa, United States, located in the central portion of the state. According to the 2022 United States Census Bureau, the county has a population of 493,378, making it the most populous county in Iowa and accounting for nearly 15% of the state's total population. The county includes the city of Des Moines, the state capital and primary urban and economic center, resulting in a high concentration of residential areas, transportation networks, and critical infrastructure within a relatively compact region. The total land area of Polk County is 1,482.5 km². Ground elevations range from approximately 228 m to 318 m above sea level, reflecting generally low-relief terrain that influences drainage patterns and flood susceptibility (Figure 1).

Polk County is bisected by the Des Moines River, the largest river system in Iowa, which originates in southwestern Minnesota and flows southeastward to the Mississippi River. Several tributaries, including Fourmile Creek, drain through the county and contribute to localized flood hazards. The area has experienced multiple significant flooding events. Between June 30 and July 1, 2018, intense thunderstorms produced heavy rainfall across central Iowa, causing major flooding within the Fourmile Creek Basin and the broader Des Moines metropolitan area. Portions of northern Polk County received 5–10 inches of precipitation, including the highest 24-hour rainfall total recorded at a National Oceanic and Atmospheric Administration weather station (National Weather Service, 2018). The resulting flood damage in Polk County exceeded $15 million, including approximately $970,000 in road and bridge repairs, with additional losses to

residential properties (O'Shea et al., 2021). The combination of dense population, concentrated infrastructure, riverine flood exposure, and documented flood impacts makes Polk County a representative setting for evaluating how social, ecological, and technological factors influence spatial patterns of flood vulnerability. This study therefore analyzes vulnerability at the census block group scale to identify areas where underlying conditions intensify potential flood impacts.

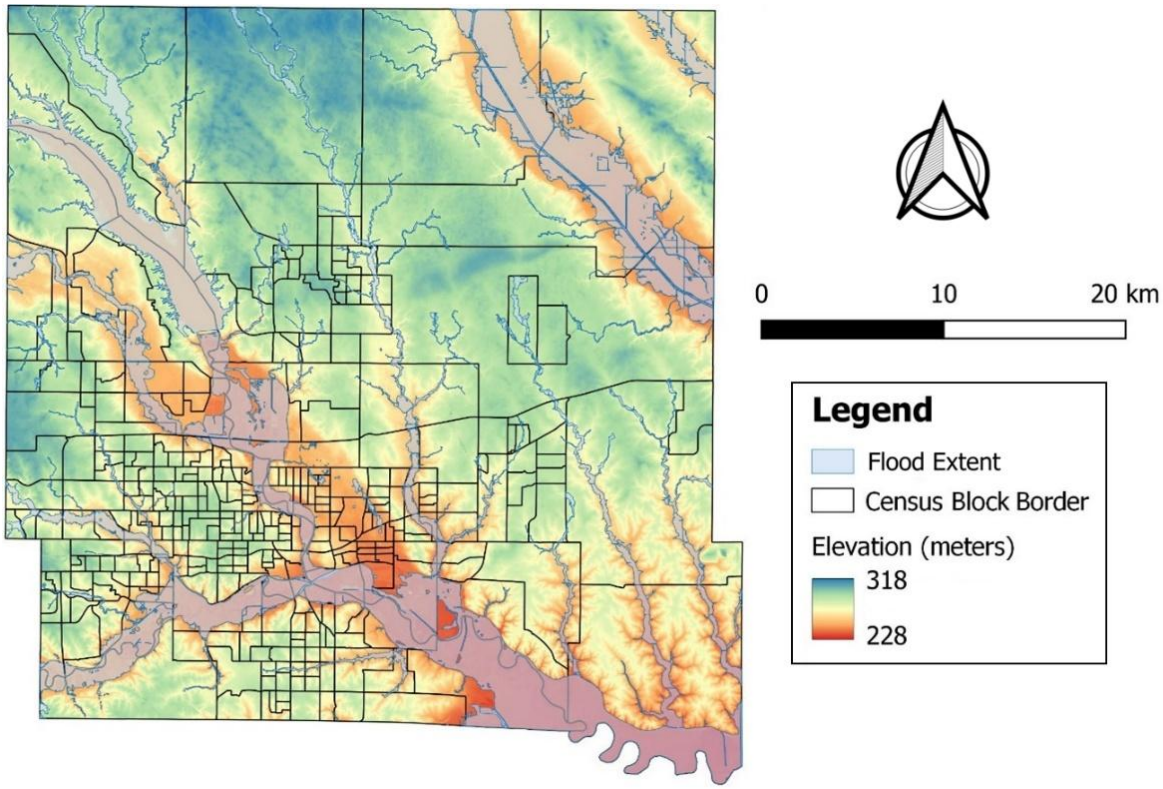

Figure 1. Census block group boundaries in Polk County overlaid with the 500-year floodplain extent and elevation surface.

2.2. Social–Ecological–Technological Systems Framework

This study employs the Social–Ecological–Technological Systems (SETS) vulnerability framework to assess flood susceptibility across Polk County. The SETS methodology was first developed by Chang et al. (2021) to evaluate vulnerability to urban floods. The SETS vulnerability framework integrates three aspects of vulnerability—namely, exposure, sensitivity, and adaptive capacity—across the domains of social, ecological, and technological that constitute urban context. This structure provides a systematic representation of the multiple factors that influence how communities experience and respond to flood hazards.

As shown in Figure 2, each domain includes two indicators for exposure, sensitivity, and adaptive capacity, resulting in six parameters per domain and 18 indicators in total. Social indicators describe demographic and socioeconomic characteristics such as population structure and renter occupancy. Ecological indicators represent terrain, land cover, and environmental conditions, including slope, proximity to toxic release inventory sites, wetlands, and vegetation

productivity (NDVI). Technological indicators capture the built environment and critical services, including roads, impervious surfaces, building density, green infrastructure, and emergency facilities. The final set of 18 variables was selected based on data availability and consistency with prior SETS-based flood vulnerability studies, particularly Chang et al. (2021) and Leta and Adugna (2023). All indicators were evaluated at the census block group (CBG) scale to maintain consistent spatial resolution across domains.

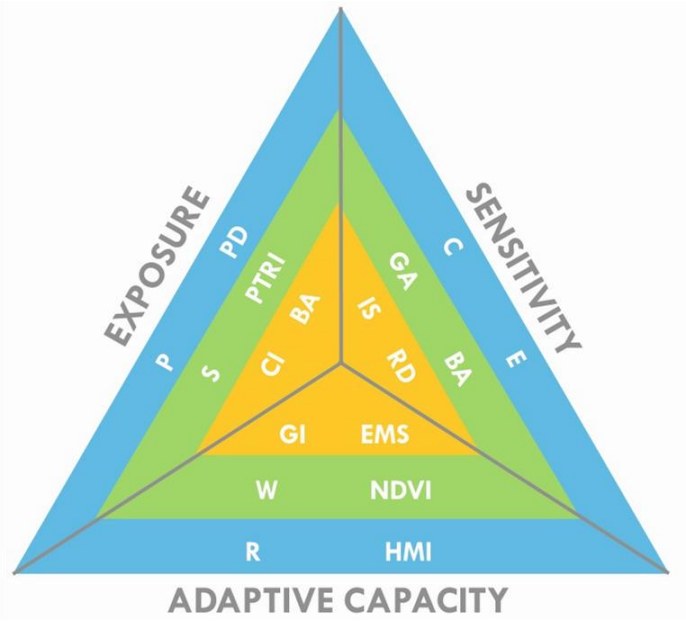

Figure 2. Conceptual diagram of the SETS flood vulnerability framework showing the 18 indicators grouped into social (blue), ecological (green), and technological (orange) domains across exposure, sensitivity, and adaptive capacity dimensions (Adapted from Chang et al. (2021)).

2.3. Data Preparation

Analyses of SETS vulnerability involve varying combinations of indicators, and no fixed or universally prescribed variable set exists for implementation (Chang et al., 2021; Pallathadka et al., 2022; Sauer, 2023). The framework requires representation across all three domains—social, ecological, and technological. The eighteen indicators defined by Chang et al. (2021) were adopted as the baseline configuration. Due to regional data limitations, seventeen of the original indicators were directly implemented, and the combined landscape metric based on shape index and average patch size was replaced with percentage of green area. Green area has been applied in both flood-related (Verma et al., 2020) and socio-ecological studies (Afriyanie et al., 2020), making it a suitable substitute within the ecological domain.

All indicators, their definitions, use cases, and corresponding data sources are documented in Table 1 to support transparency and reproducibility. All datasets were obtained from non-commercial, publicly accessible repositories. Social variables were available directly at the census block group (CBG) level, whereas ecological and technological layers were processed in QGIS tool and aggregated to CBG boundaries for spatial consistency.

Table 1. SETS vulnerability indicators, codes, definitions, and data sources used in the analysis.

Category	Parameter	Code	Source
Social Exposure	Population (total population per census block)	P (+)	ACS (2022)
	Population Density (population per unit area)	PD (+)	ACS (2022)
Social Sensitivity	Children (percentage of population under 5 years of age)	C (+)	ACS (2022)
	Elderly (percentage of population over 65 years of age)	E (+)	ACS (2022)
Social Adaptive Capacity	Renters (percentage of population living in rental housing)	R (−)	ACS (2022)
	Household Median Income	HMI (+)	ACS (2022)
Ecological Exposure	Slope (mean slope within the census block)	S (−)	Iowa DNR (2022)
	Proximity to Toxic Release Inventory (TRI) Sites (nearest-neighbor distance between centroids of parks and TRI facilities)	PTRI (+)	US Environmental Protection Agency (EPA) (2013)
Ecological Sensitivity	Green Area (proportion of green land cover within the area)	GA (−)	NLCD Land Cover (2021)
	Bare Soil (percentage of bare soil land cover within the census block)	BS (+)	NLCD Land Cover (2021)
Ecological Adaptive Capacity	Wetlands (percentage of wetland area within the census block)	W (+)	US Fish & Wildlife Service (2023)
	Vegetation Productivity (NDVI) (mean normalized difference vegetation index within the census block)	NDVI (+)	National Centers for Environmental Information (2020)
Technological Exposure	Critical Infrastructure (number of facilities such as wastewater treatment plants, public water supply facilities, and power plants within the census block)	CI (+)	US Energy Information Administration (EIA) (2024)
	Building Area (percentage of built-up area within the census block group)	BA (+)	OpenStreetMap (2015)
Technological Sensitivity	Impervious Surface (mean percentage of impervious surface within the census block group)	IS (+)	NLCD Impervious (2019)
	Road Density (total road length per unit area)	RD (+)	OpenStreetMap (2015)
Technological Adaptive Capacity	Green Infrastructure (number of green infrastructure elements per unit area)	GI (+)	City of Des Moines GIS Department (2025)
	Proximity to Emergency Management Services (EMS) (nearest-neighbor distance to hospitals, police, schools, fire, and rescue facilities)	EMS (−)	USGS National Structures (2025)

As can be obtained from Table 1, each indicator was standardized according to its assumed relationship with urban flood vulnerability, as denoted in Table 1 by positive (+) or negative (−) signs. Indicators marked with a positive sign (+) represent a direct relationship, meaning that higher values correspond to higher flood vulnerability (e.g., population density or impervious

surface). Indicators marked with a negative sign (−) represent an inverse relationship, meaning that higher values correspond to lower flood vulnerability (e.g., slope, green area, wetlands, NDVI, and emergency service proximity). Adaptive capacity indicators were treated differently from exposure and sensitivity indicators; because higher adaptive capacity reduces vulnerability, all adaptive capacity parameters were standardized using inverse scaling prior to aggregation. All indicators were ultimately expressed at the CBG level, where "area" refers to the spatial extent of each census block group.

2.4. Vulnerability Index Computation

Initially, raw indicators were standardized as percentages or densities to account for differences in census block group (CBG) size across Polk County. Demographic variables (e.g., children, elderly population, women, and tenants) were expressed as proportions of the total CBG population, whereas environmental and infrastructure variables were converted to percentages or densities relative to CBG area. This conversion removes the influence of unit size and allows direct comparison among spatial units. The derived parameter values were then normalized to a common range between 0 and 1. Normalization rescales variables to the same numerical interval so that indicators with different units and magnitudes contribute comparably during aggregation (Hossein Javaheri, 2008). For parameters positively related to urban flood vulnerability, normalization was performed using Equation 1:

$$V_{P\,(+)} = \frac{X_P - X_{Pmin}}{X_{Pmax} - X_{Pmin}} \qquad \text{Eq. 1}$$

where V_P is the normalized value of parameter P, X_P is the original parameter value, X_{Pmin} and X_{Pmax} represent the minimum and maximum observed values of that parameter. On the other hand, for inversely related to urban flood vulnerability parameters (e.g., higher slope reduces flood vulnerability), the transformation was reversed using Equation 2:

$$V_{P\,(-)} = \frac{X_{Pmax} - X_P}{X_{Pmax} - X_{Pmin}} \qquad \text{Eq. 2}$$

This step aligns all indicators directionally so that higher normalized values consistently represent higher vulnerability. The normalized indicators were subsequently aggregated to calculate domain-specific vulnerability scores for the social, ecological, and technological systems using Equation 3:

$$V_{domain} = \frac{E_1 + E_2 + S_1 + S_2}{AC_1 + AC_2} \qquad \text{Eq. 3}$$

where E_1 and E_2 represent exposure parameters, S_1 and S_2 represent sensitivity parameters, and AC_1 and AC_2 represent adaptive capacity parameters. and AC_2 is adaptive capacity parameter 2. The composite social V_S, ecological V_E, and technological V_E, scores were normalized again prior to combination. Pairwise and integrated indices were then computed using Equations 4–7:

$$V_{SE} = \frac{V_S + V_E}{2} \quad \text{Eq. 4}$$

$$V_{ET} = \frac{V_E + V_T}{2} \quad \text{Eq. 5}$$

$$V_{ST} = \frac{V_S + V_T}{2} \quad \text{Eq. 6}$$

$$V_{SET} = \frac{V_S + V_E + V_T}{3} \quad \text{Eq. 7}$$

All calculated scores were joined to the CBG spatial layer in QGIS to generate the corresponding vulnerability maps. Flood hazard layers were incorporated later for spatial comparison and interpretation.

2.5. Statistical Evaluation and Spatial Consistency

Statistical analyses were performed to assess the behavior, interpretability, and robustness of the developed vulnerability indices and to investigate the relationship between composite SET scores and independently observed flood exposure. The purpose of these analyses was to confirm that the indices characterize intrinsic socio-ecological and infrastructural susceptibility rather than merely replicating the spatial extent of inundation, and to determine whether the composite formulation is dominated by any individual indicator or remains stable under sampling variability.

Linear associations between variables were quantified using Pearson's correlation coefficient. Correlations were computed between the composite SET score and two measures of flood exposure at the census block group scale, including the proportion of inundated area and a binary indicator of flood presence, as well as between the SET score and each normalized input parameter. Pearson correlation was adopted because all indicators were continuous, standardized to a common scale, and suitable for parametric association analysis (Duran & Demir, 2026). The coefficient r is calculated as Equation 8:

$$r = \frac{\sum(x_i - \bar{x})(y_i - \bar{y})}{\sqrt{\sum(x_i - \bar{x})^2 \sum(y_i - \bar{y})^2}} \quad \text{Eq. 8}$$

where x_i and y_i represent paired observations and $\bar{x}$ and $\bar{y}$ are the corresponding sample means. The coefficient ranges from −1 to 1 and describes both the direction and strength of association. These correlations were used to determine whether the vulnerability surface aligns with flood exposure and to evaluate the relative influence of individual indicators on the composite score.

Uncertainty in the correlation estimates was addressed through confidence intervals derived from Fisher's z-transformation (Fisher, 1915; Zou, 2007). The transformation and associated standard error are defined in Equation 9 and 10:

$$z = \frac{1}{2} ln\left(\frac{1-r}{1+r}\right);\ SE = \frac{1}{\sqrt{n-3}} \qquad \text{Eqs. 9, 10}$$

where z represents the Fisher-transformed correlation and SE denotes the corresponding standard error. For a 95% confidence interval, the lower and upper bounds of z are obtained by using Equation 11 and 12:

$$z_{low} = z - 1.96 * SE;\ z_{high} = z + 1.96 * SE \qquad \text{Eqs. 11, 12}$$

where 1.96 is the critical value of the standard normal distribution for the 95% probability level. These bounds are subsequently converted back to the correlation scale using Equation 13 and 14:

$$r_{low} = \frac{e^{2(z_{low})} - 1}{e^{2(z_{low})} + 1};\ r_{high} = \frac{e^{2(z_{high})} - 1}{e^{2(z_{high})} + 1} \qquad \text{Eqs. 13, 14}$$

This resampling framework offers a distribution-free assessment of variability and facilitates the comparison of consistency among individual, paired, and composite indices in relation to flood exposure indicators. Wider intervals show more heterogeneity or susceptibility to sample fluctuation, while narrower intervals show consistent scores throughout the study area. Flood variables were treated exclusively as independent exposure measures and were not incorporated into index construction. This separation ensures that statistical comparisons evaluate complementarity between susceptibility and hazard rather than circular dependence. Collectively, the correlation and bootstrap analyses provide quantitative evidence of independence, multi-indicator balance, and stability of the SET vulnerability framework.

3. Results and Discussion

This section presents the spatial and statistical results of the vulnerability assessment and identifies census block groups (BGs) in Polk County that exhibit elevated susceptibility to flood impacts across social, ecological, and technological dimensions. Results are organized progressively, beginning with domain-specific (singular) vulnerability patterns, followed by composite indices that capture interactions among domains, and concluding with statistical analyses that evaluate relationships with observed flood exposure and the stability of the scoring framework. All

vulnerability scores are visualized using a five-class Natural Breaks (Jenks) classification scheme (very low to very high). The class boundaries are determined by minimizing variance within classes while maximizing differences between classes, thereby grouping block groups with similar score magnitudes and emphasizing meaningful spatial contrasts in the distribution of vulnerability. Such classification has been shown to improve interpretability of vulnerability mapping by reflecting inherent structures in the data rather than imposing arbitrary intervals (Noori et al., 2023).

To interpret how intrinsic vulnerability relates to hydraulic hazard, all vulnerability maps are evaluated alongside the 500-year floodplain extent. The floodplain is treated as an independent measure of exposure and is not incorporated into the vulnerability calculations themselves, allowing direct comparison between where inundation occurs and where susceptibility is highest. Flood hazard delineation is obtained from the Iowa Flood Information System (IFIS; Demir et al., 2018). Although the 100-year floodplain is commonly used for regulatory planning, the 500-year scenario is adopted here to represent more extreme and low-probability events that better reflect potential future conditions under changing climate and land-use patterns.

3.1. Domain-Specific Vulnerability (Singular Scores)

Domain-specific scores for the social (S), ecological (E), and technological (T) domains were evaluated separately to identify how each system contributes to spatial vulnerability patterns before aggregation. Examining each domain separately clarifies how demographic sensitivity, environmental buffering capacity, and built-environment and service accessibility contribute differently to spatial risk patterns. To support interpretation relative to hazard conditions, domain maps were compared with the 500-year floodplain extent to assess whether elevated vulnerability systematically coincides with areas of potential inundation or instead reflects broader structural susceptibility independent of direct exposure.

The three domains exhibit distinctly different spatial organizations and statistical signatures, confirming that vulnerability is multi-dimensional rather than spatially coincident across systems. Under natural breaks classification into five classes, block groups categorized as high or very high vulnerability account for 13.4% (n = 45) of areas in the social domain, 11.0% (n = 37) in the ecological domain, and only 6.8% (n = 23) in the technological domain. This reduction indicates that elevated technological vulnerability is more spatially selective, whereas social and ecological sensitivities are more broadly distributed.

The social vulnerability surface (Figure 3a) is comparatively homogeneous and broadly distributed, with higher scores occurring in the city center and portions of the western urban corridor but without strong spatial clustering. Statistical contrasts indicate that these elevated scores are not associated with larger total populations, as mean population counts remain nearly unchanged relative to county averages. Instead, social vulnerability is driven by socioeconomic composition. Block groups classified as high or very high show a marked reduction in median household income of approximately 45% compared to the county mean, accompanied by a more than 150% increase in renter occupancy and a 35% increase in the proportion of children.

Population concentration also increases substantially, indicating denser residential conditions. Elderly proportions change only modestly, suggesting that vulnerability is more strongly related to economic constraints and housing tenure instability than to aging alone. These patterns collectively reflect reduced financial resilience, higher dependency burdens, and limited recovery capacity.

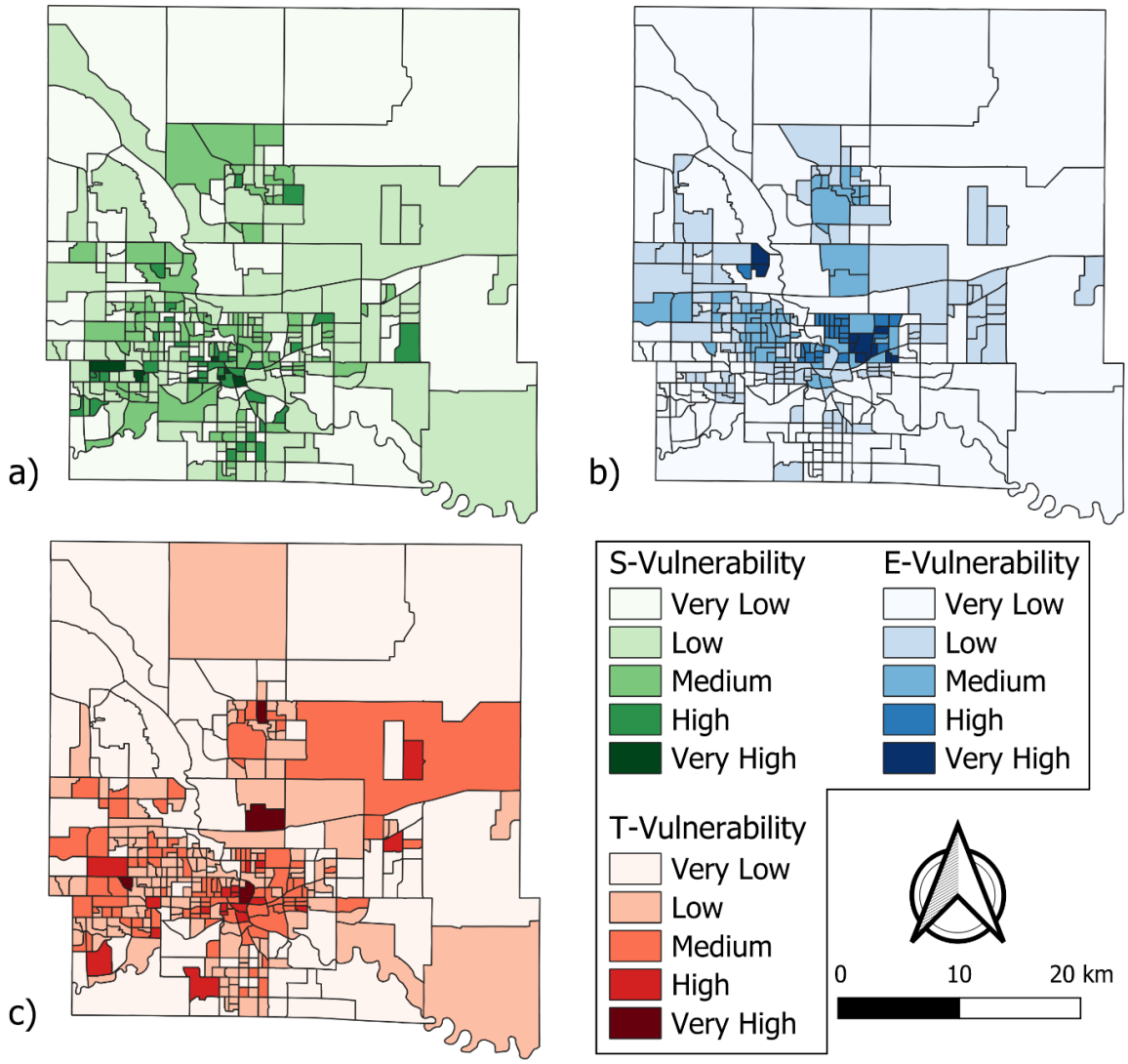

Figure 3. Domain-specific vulnerability maps at the census block group scale for Polk County: (a) Social (S), (b) Ecological (E), and (c) Technological (T).

Ecological vulnerability (Figure 3b) displays a markedly different and more heterogeneous structure. High scores concentrate in densely developed areas, particularly along the urban corridor and near the downtown core, forming contiguous zones shaped by land cover and terrain characteristics. Compared with county-wide means, block groups in the high and very high classes exhibit substantial reductions in ecological buffering indicators. Wetland coverage decreases by

nearly 97%, green area percentages decline by approximately two-thirds, and vegetation productivity measured by NDVI drops by more than 60%. These areas are also characterized by flatter terrain and increased impervious surfaces and reduced infiltration capacity. In contrast, areas with greater vegetation, higher wetland presence, and more heterogeneous terrain consistently fall into lower vulnerability classes. The ecological domain therefore reflects the loss of natural protective functions and the intensification of urban land cover, highlighting how landscape modification diminishes environmental resilience to flooding and other hydrologic disturbances.

Technological vulnerability (Figure 3c) shows the most spatially selective pattern, with elevated scores concentrated in the urban core and several northern block groups. This distribution reflects localized concentrations of infrastructure and uneven access to emergency services rather than a simple urban–rural gradient. High and very high technological block groups exhibit pronounced increases in built-environment indicators, including more than a doubling of building area and critical infrastructure counts, and substantially reduced proximity to emergency services. These characteristics indicate environments with dense physical assets that are both highly exposed to disruption and constrained in their adaptive capacity. The combination of larger infrastructure inventories and limited response accessibility elevates the likelihood of service interruption and cascading impacts during extreme events. Consequently, technological vulnerability identifies areas where functional disruption risks are amplified, even when demographic or ecological sensitivity may be comparatively lower.

Flood exposure exhibits greater spatial heterogeneity than any of the singular vulnerability domains and does not systematically coincide with areas classified as socially, ecologically, or technologically vulnerable. Block groups identified as high vulnerability frequently correspond to average or below-average proportions of mapped floodplain coverage, while some extensively inundated areas display comparatively low intrinsic susceptibility. This inconsistency highlights the fundamental distinction between exposure and vulnerability. The floodplain delineates where inundation occurs, whereas the domain-specific indices characterize the underlying sensitivity and adaptive capacity of populations, ecosystems, and infrastructure, thereby indicating the severity of consequences if flooding occurs. Treating these concepts as equivalent risks misidentification because hazard presence alone does not determine impact severity.

Considered together, the singular domain results provide complementary insights into different dimensions of flood vulnerability. Social scores highlight socioeconomic sensitivity, ecological scores reflect reduced natural buffering capacity, and technological scores capture infrastructure concentration and service-access limitations. Because these patterns only partially overlap, no single domain fully represents overall risk, supporting the use of composite indices to describe cumulative susceptibility.

3.2. Composite Vulnerability Indices

Composite indices evaluate where vulnerabilities co-occur and interact across systems. These combined indices identify locations where multiple dimensions of susceptibility intersect, creating

conditions in which social sensitivity, ecological degradation, and infrastructure limitations compound rather than act independently. Such overlap is particularly important for flood risk assessment, as simultaneous stresses across systems can intensify impacts, slow response, and hinder recovery. To examine these interactions progressively, paired combinations of domains (S–E, E–T, and S–T) were first evaluated, followed by the comprehensive SET index integrating all three components.

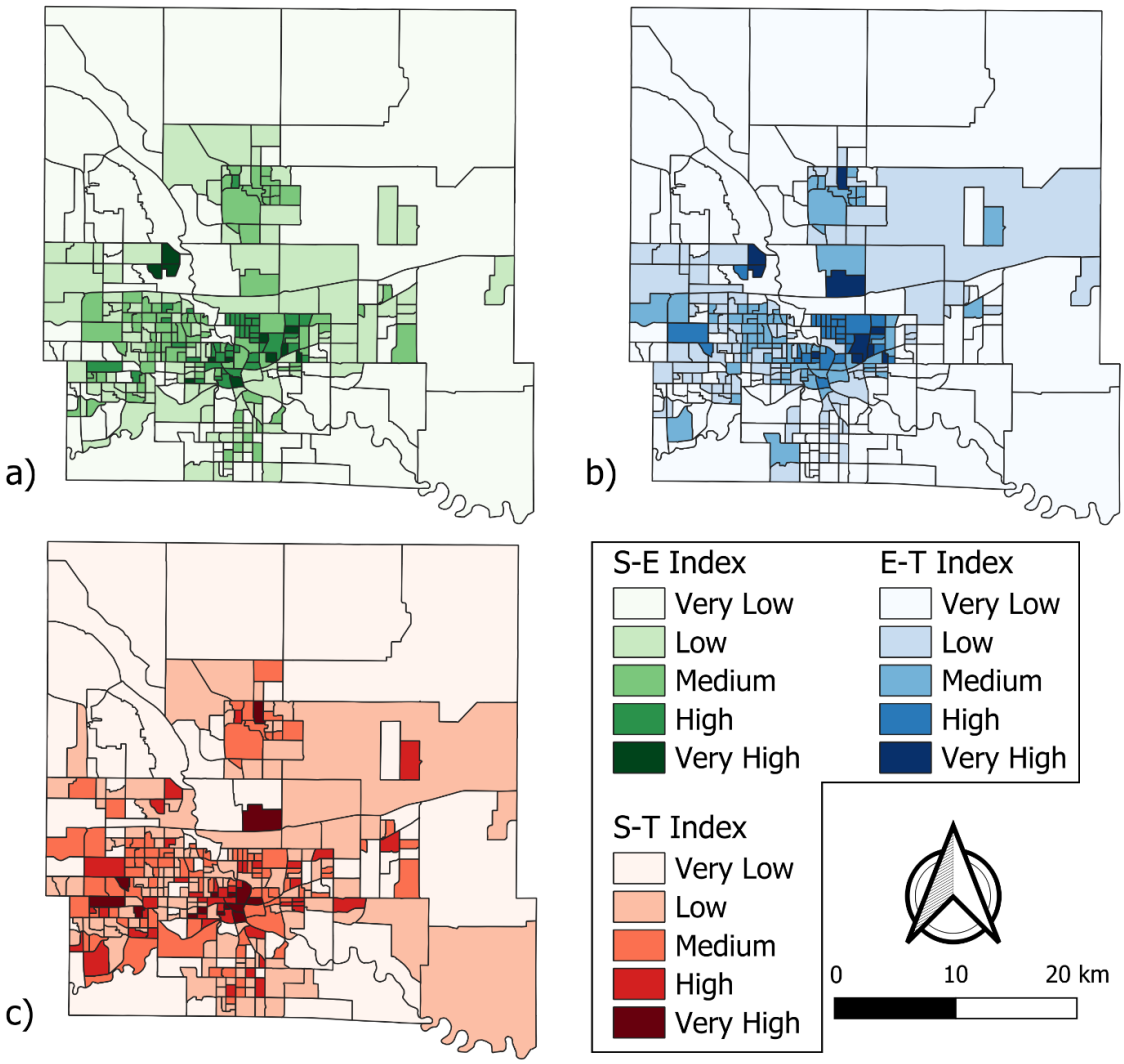

Figure 4. Paired composite vulnerability indices for Polk County: (a) Social–Ecological (S-E), (b) Ecological–Technological (E-T), and (c) Social–Technological (S-T).

The three paired indices exhibit broader and more contiguous areas of elevated vulnerability than the singular domains, reflecting the accumulation of multiple stressors. High and very high classes account for 16.1% of block groups in SE (n = 54), 12.2% in ET (n = 41), and 17.9% in ST (n = 60), indicating that coupling domains consistently expands the extent of identified hotspots relative to individual scores.

The SE combination (Figure 4a) is strongly concentrated along the city center and the main river corridor, with moderate extension into western neighborhoods and consistently lower scores across the northern and eastern portions of the county. This pattern reflects the interaction between socioeconomic disadvantages and reduced ecological buffering. Block groups in the high SE class exhibit pronounced reductions in median household income, averaging more than one-third below the county mean, together with renter occupancy exceeding 65% and higher population density. Ecological capacity indicators decline simultaneously. Green space and wetlands decrease by 70–95%, and vegetation productivity is markedly lower. These conditions indicate locations where socially sensitive populations coincide with heavily modified landscapes that provide limited natural flood mitigation, resulting in compounded rather than isolated vulnerability.

The ET index (Figure 4b) shows a distinctly different configuration, with clustered hotspots in the downtown core and north of the city center, weaker expression toward the western corridor, and localized highlights in eastern agricultural areas. Compared with SE, this pairing emphasizes the interaction between landscape modification and infrastructure intensity. High ET block groups display substantial increases in impervious surface, building area, and road density, accompanied by reductions in slope, wetlands, and vegetative cover. Critical infrastructure counts remain similar to or slightly above county averages, and emergency service proximity varies. These results indicate that exposure of physical assets, rather than social characteristics alone, drives the composite score. The pattern therefore identifies areas where degraded ecological function and dense built systems coincide, creating environments that are both hydrologically sensitive and operationally vulnerable.

In contrast, the ST combination (Figure 4c) shows the most spatially diffuse and homogeneous pattern among the paired indices. Elevated scores extend across western neighborhoods, several northern block groups, and parts of the southern and eastern agricultural regions, including larger rural blocks that do not appear prominently in the SE or ET maps. This broader footprint reflects the coupling of socioeconomic sensitivity with infrastructure and service-access constraints. High ST block groups exhibit strong reductions in income, renter proportions that double relative to county averages, and increases in children and population concentration, while also showing substantial growth in building coverage, impervious surfaces, and longer distances to emergency facilities. The interaction of limited adaptive capacity and greater dependence on physical infrastructure produces vulnerability that is not confined to the urban core, explaining the more distributed appearance of the ST surface.

Overall, the paired composites demonstrate that vulnerability patterns shift according to which systems are combined. Each pairing highlights different hotspots rather than simply reinforcing the singular maps. To capture the cumulative effect of all domains simultaneously, a comprehensive index integrating social, ecological, and technological components was subsequently developed.

As shown in Figure 5, SET index identifies an extensive pattern of compound vulnerability, with high and very high classes encompassing 20% of all block groups (n = 67), the largest share among all scenarios. Spatially, the SET surface closely resembles the ET pattern but with stronger

intensification in the city center and along the primary river corridor, where darker and more continuous clusters emerge. These areas combine lower household income and higher renter presence with limited vegetation, reduced wetlands, extensive impervious cover, dense building footprints, and concentrations of critical infrastructure. The simultaneous degradation of social capacity, ecological buffering, and technological resilience produces cumulative susceptibility that exceeds any single or paired domain.

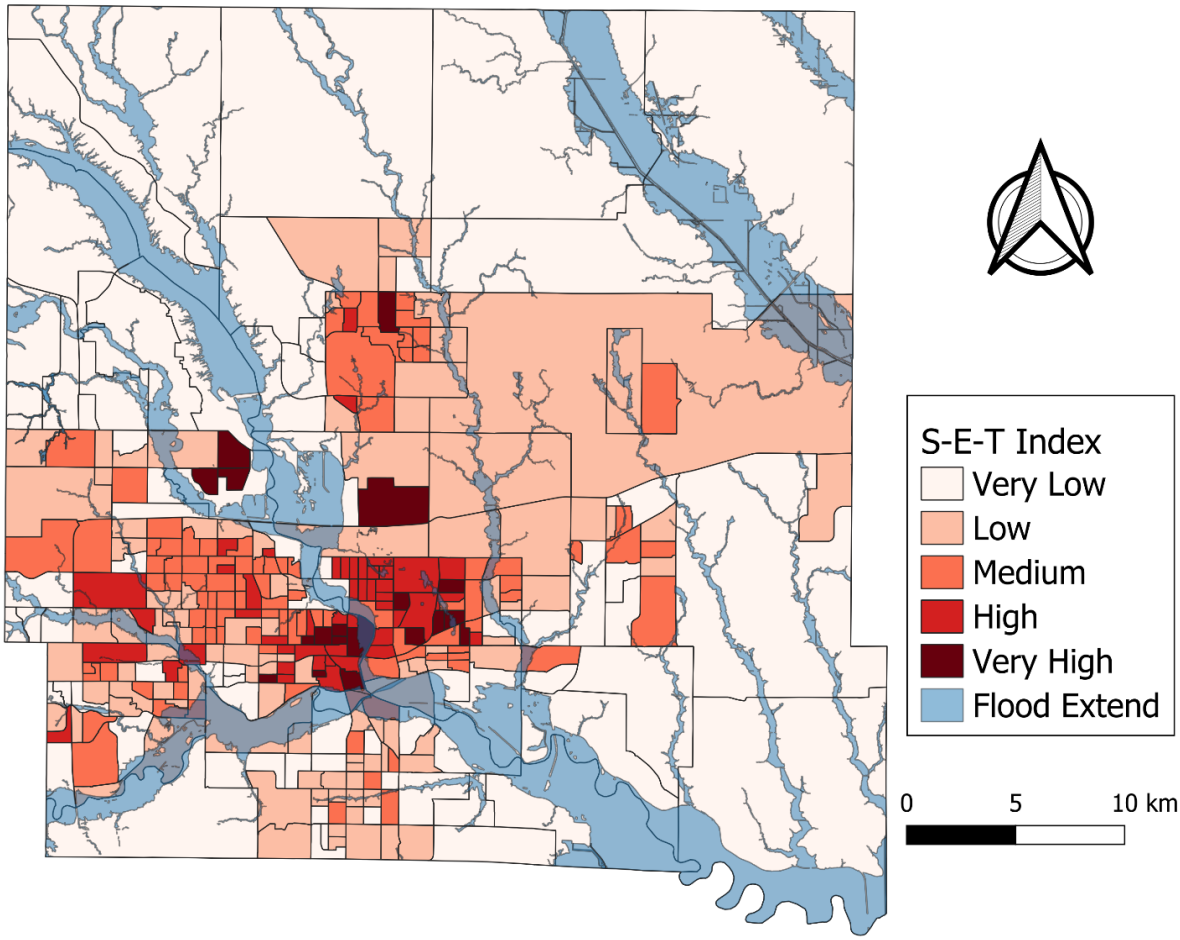

Figure 5. Integrated S-E-T composite vulnerability index at the census block group scale with 500-year floodplain overlay.

When compared with the floodplain overlay, SET highlights locations where intrinsic susceptibility and physical exposure intersect most clearly. Several high and very high SET block groups coincide with inundation branches along the river corridor and urbanized sections of Des Moines, while additional susceptible areas appear in peripheral agricultural regions where large block groups combine service-access limitations and reduced environmental buffering. The contrast between tightly bounded flood extents and the broader distribution of SET scores reinforces that hazard exposure alone does not define risk, but that the most consequential impacts occur where exposure overlaps with compounded multi-domain vulnerability.

Overall, the composite analysis confirms that vulnerabilities across social, ecological, and technological systems interact in non-linear ways. Each domain contributes distinct information, and their integration reveals hotspots that are not identifiable from singular assessments alone. The SET index therefore provides a more comprehensive representation of cumulative flood risk by combining complementary dimensions of susceptibility into a unified framework.

3.3. Statistical Validation and Spatial Consistency

This section presents statistical analyses used to examine relationships between the SET index, flood exposure, and individual indicators. Correlation measures are reported to summarize these relationships and to examine the consistency and stability of the resulting vulnerability scores. The relationship between the SET index and observed flood conditions was examined using Pearson correlations between continuous SET scores and two flood exposure measures at the census block group scale: the proportion of inundated area within each block group and a binary indicator of flood presence. These flood variables represent hydraulic hazard and were not used in constructing the SET index. It provides an independent basis for comparison. Of the 336 census block groups in Polk County, 185 (55%) intersect the 500-year floodplain, and among those exposed groups the average inundated area is 17.43%, indicating that flooding is spatially widespread but typically affects only a fraction of each block group rather than the entire unit.

The mean SET score across all block groups is 0.206, whereas the mean score for flooded groups is lower (0.181), resulting in weak-moderate negative correlations with flood extent ($r = -0.27$) and flood presence ($r = -0.29$). This inverse association indicates that the SET index does not mirror the floodplain footprint. Instead, it captures socio-ecological and infrastructural conditions that are distinct from hydraulic exposure. The moderate negative correlation indicates that the SET index captures susceptibility patterns that are independent of the floodplain footprint rather than simply reproducing inundation boundaries.

To assess how individual indicators contribute to the composite SET score, Pearson correlations were computed between the SET index and each normalized parameter (Table 2). The variables represent exposure, sensitivity, and adaptive capacity across the social, ecological, and technological domains. Because parameters were scaled according to their assumed direction of influence, the sign of each coefficient reflects this normalization. Variables coded inversely during aggregation can therefore exhibit negative correlations without indicating lower importance; instead, the negative sign shows that their spatial distribution contrasts with the final SET surface.

The correlation analysis shows that the composite SET surface aligns most strongly with parameters describing urban development intensity and built-environment concentration, which are related to impervious cover, road density, building area, and population density show the highest positive associations with the index, demonstrating that areas characterized by dense urban form tend to coincide with elevated composite vulnerability. In contrast, several environmental and socioeconomic indicators exhibit inverse relationships, reflecting their normalization direction and spatial structures that differ from the dominant urban clusters rather than diminished importance within the model.

Table 2. Pearson correlation coefficients between normalized indicators and the composite SET vulnerability index.

Indicator	r
Population	−0.09
Population density	0.57
Children	0.15
Elderly	0.02
Median income	−0.43
Renters	−0.42
Slope	0.29
Proximity to TRI	−0.04
Green area	0.18
Bare soil	−0.28
Wetlands	−0.42
NDVI	−0.39
Critical infrastructure	−0.13
Building area	0.45
Impervious surface	0.66
Road density	0.54
Green infrastructure density	0.11
Proximity to emergency centers	−0.15

More importantly, correlation coefficients remain moderate rather than extreme across all parameters. No single indicator demonstrates a dominant association with the SET score. This pattern supports the idea that the composite index is not controlled by any individual variable or subsystem but instead reflects the combined influence of social, ecological, and technological conditions acting together. Statistical behavior therefore shows the intended multi-indicator formulation, in which vulnerability emerges from the interaction of several contributing factors rather than from a single controlling driver. Finally, the stability and variability of the domain-level and composite vulnerability scores, as well as flood coverage, were evaluated using bootstrap resampling, and the resulting means and 95% confidence intervals are summarized in Table 3.

According to Table 3, across the three primary domains, the Social Index exhibits the narrowest dispersion. This pattern reflects the smoother spatial distribution of socioeconomic characteristics, which vary less abruptly across the county. In contrast, the Ecological Index shows the widest confidence intervals, revealing greater heterogeneity in land cover, vegetation, and terrain conditions. These environmental attributes change sharply between urbanized and natural areas, producing larger spatial contrasts and higher variability in the resulting scores. The Technological Index displays intermediate behavior, with variability greater than the social component but lower than the ecological one, consistent with the localized clustering of infrastructure and service accessibility. When domains are combined, variability decreases rather than increases. The paired

indices (SE, ET, and ST) exhibit spreads that are comparable to or smaller than their respective singular components, and the final SET composite shows the smallest relative interval width overall. This reduction shows that aggregation dampens localized extremes across domains and produces more stable and balanced estimates. In practical terms, integrating multiple dimensions smooths isolated fluctuations and yields a more robust representation of underlying vulnerability patterns.

Table 3. Bootstrap computation and 95% confidence intervals for singular, paired, composite vulnerability indices, and flood exposure metrics.

Index / Metric	Sample Size (N)	Mean	95% CI (Lower)	95% CI (Upper)	CI Width	Relative Width (%)
S	336	0.242	0.229	0.256	0.027	11.0
E	336	0.214	0.197	0.234	0.037	17.4
T	336	0.163	0.152	0.175	0.023	14.1
SE	336	0.228	0.216	0.241	0.025	10.9
ET	336	0.189	0.176	0.200	0.024	12.8
ST	336	0.203	0.192	0.213	0.021	10.4
Composite SET	336	0.206	0.196	0.217	0.021	10.2
Flood Coverage (%)	185	17.434	14.358	20.519	6.161	35.3

Flood coverage exhibits a distinct behavior. By computing only for block groups intersecting the floodplain (N = 185), it presents substantially wider confidence intervals than any vulnerability index. This broader spread reflects the fragmented and irregular geometry of inundation, where adjacent block groups can experience markedly different flood extents. Unlike the smoother socio-ecological and technological indicators, which change gradually across space, flood exposure is inherently discontinuous and controlled by channel morphology and local topography. Consequently, while the vulnerability indices remain statistically consistent across resamples, flood coverage varies sharply between locations. These results demonstrate that vulnerability and exposure capture distinct processes and should be evaluated separately rather than treated as interchangeable measures.

4. Conclusion

This study developed and applied a Social–Ecological–Technological Systems (SETS) framework to evaluate flood vulnerability across census block groups in Polk County, Iowa. By separating vulnerability into social, ecological, and technological domains and then integrating them through paired and composite indices, the analysis demonstrated that flood risk is multidimensional and cannot be represented by hazard exposure or any single subsystem alone. Each domain revealed distinct spatial patterns and statistical behavior. These differences show that demographic conditions, environmental buffering, and infrastructure characteristics influence flood impacts through separate pathways.

Domain-specific results showed that social vulnerability is broadly distributed and primarily associated with lower income and higher renter occupancy. Ecological vulnerability follows patterns of land-cover modification and reduced natural buffering along the urban core and river corridor. Technological vulnerability concentrates around dense infrastructure and service-access constraints that increase the likelihood of functional disruption. When domains were combined, additional hotspots appeared that were not visible in singular maps. This outcome demonstrates that interacting weaknesses intensify impacts and that isolated indicators cannot capture cumulative risk.

Instead of producing isolated scores, the SETS framework clarified where different vulnerability mechanisms converge within Polk County. In Des Moines, the highest composite scores cluster along the downtown corridor and the Des Moines River, where lower-income renter populations coincide with limited ecological buffering and dense impervious infrastructure. Additional hotspots emerge in northern and eastern peripheral block groups, where service accessibility and infrastructure constraints elevate technological vulnerability despite lower population density. These location-specific patterns demonstrate how combining domains reveals compounded susceptibility that is not evident from hazard maps or singular indicators alone. The framework therefore functions as a practical planning tool, allowing local agencies to prioritize neighborhoods and infrastructure systems based on the dominant drivers of risk in each area rather than relying on a single uniform metric.

The analysis has several methodological considerations. Flood exposure was represented using a static 500-year floodplain that delineates potential inundation extent but does not explicitly account for event dynamics such as depth, duration, timing, or compound drainage and infrastructure interactions. As a result, the flood layer characterizes spatial exposure rather than the full temporal progression of impacts. Several indicators are derived from census and land-cover datasets aggregated at the census block group scale, which supports countywide planning while smoothing fine-scale variability within individual neighborhoods. Finally, the index formulation summarizes complex social, ecological, and technological processes into normalized indicators and composite scores. This structure improves transparency and comparability while focusing the analysis on measurable spatial conditions, whereas behavioral, institutional, and site-specific factors remain outside the present scope.

Future work should advance the framework both technically and operationally. Incorporating more sophisticated flood modeling approaches, including depth-dependent hydraulic simulations, time-varying inundation dynamics, and scenario-based climate projections, would enable estimation of impact magnitude and duration rather than exposure extent alone. Coupling the SETS indicators with formal multi-criteria decision-making methods, such as AHP or fuzzy AHP, would support more systematic weighting and sensitivity analysis tailored to stakeholder needs. Expanding the platform into interactive informatics tools or web-based decision-support systems (Demir & Beck, 2009) could further enhance accessibility for planners and community agencies, allowing real-time exploration of vulnerability patterns and scenario testing. Applying the framework across multiple cities and scales would also strengthen generalizability and facilitate

comparative resilience planning. Overall, this study presents a structured and adaptable approach for understanding flood vulnerability beyond hazard boundaries. The SETS framework enables integrated, data-driven decision making and offers a practical foundation for building more resilient communities.

References

Afriyanie, D., Julian, M. M., Riqqi, A., Akbar, R., Suroso, D. S. A., & Kustiwan, I. (2020). Re-framing urban green spaces planning for flood protection through socio-ecological resilience in Bandung City, Indonesia. *Cities*, 101, 102710. https://doi.org/10.1016/j.cities.2020.102710.

Agliamzanov, R., Sit, M., & Demir, I. (2020). Hydrology@ Home: a distributed volunteer computing framework for hydrological research and applications. *Journal of Hydroinformatics*, *22*(2), 235-248.

Alabbad, Y., & Demir, I. (2024). Geo-spatial analysis of built-environment exposure to flooding: Iowa case study. *Discover Water*, *4*(1), 28.

Alabbad, Y., & Demir, I. (2025). Understanding flood risk in public transit systems: Insights from accessibility and vulnerability analysis in Iowa. *International journal of disaster risk reduction*, *126*, 105615.

Alabbad, Y., Mount, J., Campbell, A. M., & Demir, I. (2024). A web-based decision support framework for optimizing road network accessibility and emergency facility allocation during flooding. *Urban Informatics*, 3(1), 10. https://doi.org/10.1007/s44212-024-00040-0.

Bixler, R. P., Lieberknecht, K., Leite, F., Felkner, J., Oden, M., Richter, S., Atshan, S., Zilveti, A., & Thomas, R. F. (2019). An Observatory Framework for Metropolitan Change: Understanding Urban Social–Ecological–Technical Systems in Texas and Beyond. *Sustainability*, 11(13), 3611. https://doi.org/10.3390/su11133611.

Chang, H., Franczyk, J., & Kim, C. (2008). What is responsible for increasing flood risks? The case of Gangwon Province, Korea. Natural Hazards, 48(3), 339–354.

Chang, H., Pallathadka, A., Sauer, J., Grimm, N. B., Zimmerman, R., Cheng, C. J., Iwaniec, D. M., Kim, Y., Lloyd, R., McPhearson, T., Rosenzweig, B., Troxler, T. G., Welty, C., Brenner, R., & Herreros-Cantis, P. (2021). Assessment of urban flood vulnerability using the social-ecological-technological systems framework in six US cities. Sustainable Cities and Society, 68, 102786. https://doi.org/10.1016/j.scs.2021.102786.

Cikmaz, B. A., Yildirim, E., & Demir, I. (2023). Flood susceptibility mapping using fuzzy analytical hierarchy process for Cedar Rapids, Iowa. *International Journal of River Basin Management*, 1-13. https://doi.org/10.1080/15715124.2023.2216936.

City of Des Moines GIS Department. (2024). City of Des Moines GIS Data Portal. Public spatial datasets. Accessed 2024. https://data.dsm.city/.

Cinner, J. E., Huchery, C., Darling, E. S., Humphries, A. T., Graham, N. a. J., Hicks, C. C., Marshall, N., & McClanahan, T. R. (2013). Evaluating social and ecological vulnerability of coral reef fisheries to climate change. PLOS ONE, 8(9), e74321.

De Brito, M. M., Evers, M., & Almoradie, A. (2018). Participatory flood vulnerability assessment: a multi-criteria approach. Hydrology and Earth System Sciences, 22(1), 373–390. https://doi.org/10.5194/hess-22-373-2018.

Demir, I., & Beck, M. B. (2009, April). GWIS: a prototype information system for Georgia watersheds. In *Georgia Water Resources Conference: Regional Water Management Opportunities, UGA, Athens, GA, US*.

Demir, I., Yildirim, E., Sermet, Y., & Sit, M. A. (2018). FLOODSS: Iowa flood information system as a generalized flood cyberinfrastructure. *International journal of river basin management*, *16*(3), 393-400.

Dewitz, J., 2023, National Land Cover Database (NLCD) 2021 Products: U.S. Geological Survey data release, https://doi.org/10.5066/P9JZ7AO3.

Dirmeyer, P. A., & Kinter III, J. L. (2010). Floods over the US Midwest: A regional water cycle perspective. Journal of Hydrometeorology, 11(5), 1172-1181. https://doi.org/10.1175/2010JHM1196.1.

Duran, E., Alabbad, Y., Mount, J., Yildirim, E., & Demir, I. (2025a). Comprehensive analysis of riverine flood impact on bridge and transportation network: Iowa case study. *International Journal of River Basin Management*, 1-14. doi.org/10.1080/15715124.2025.2457546.

Duran, E., & Demir, I. (2026). Enhancing the Resilience of Wind Energy Infrastructure in Iowa: Flood Risk Assessment and Site Suitability Analysis for Critical Infrastructure Protection. *International Journal of Disaster Risk Reduction*, 106003. doi.org/10.1016/j.ijdrr.2026.106003.

Duran, E., Mount, J., & Demir, I. (2025b). Comprehensive Flood Impact Assessment for Iowa Bridge Infrastructure Using Integrated AHP and Fuzzy AHP Analysis. *EarthArXiv*, https://doi.org/10.31223/X5VD9Q.

Duran, E., Mount, J., & Demir, I. (2025c). IBIS: A Community-Oriented Framework for Flood-Induced Bridge Vulnerability Assessment and Prioritization for Iowa. *EarthArxiv*, https://doi.org/10.31223/X5CT9H.

Ebert-Uphoff, I., Thompson, D.R., Demir, I., Gel, Y.R., Karpatne, A., Guereque, M., Kumar, V., Cabral-Cano, E. and Smyth, P., (2017, September). A vision for the development of benchmarks to bridge geoscience and data science. In *17th international workshop on climate informatics*.

Hossein Javaheri, S. (2008). Response modeling in direct marketing: a data mining based approach for target selection.

Huang, H., Fischella, M. R., Liu, Y., Ban, Z., Fayne, J. V., Li, D., Cavanaugh, K. C., & Lettenmaier, D. P. (2022). Changes in mechanisms and characteristics of western US floods over the last sixty years. Geophysical Research Letters, 49(3). Portico. https://doi.org/10.1029/2021gl097022.

Iowa Department of Natural Resources. (2022). Iowa 30-meter digital elevation model (DEM) [Raster dataset]. www.iowadnr.gov. Iowa Geospatial Data. State of Iowa Open Geospatial Data. Retrieved from https://geodata.iowa.gov/.

Kemter, M., Marwan, N., Villarini, G., & Merz, B. (2023). Controls on flood trends across the United States. Water Resources Research, 59(2). https://doi.org/10.1029/2021wr031673

Krajewski, W. F., Ghimire, G. R., Demir, I., & Mantilla, R. (2021). Real-time streamflow forecasting: AI vs. Hydrologic insights. *Journal of Hydrology X*, *13*, 100110.

Lauerburg, R. a. M., Diekmann, R., Blanz, B., Gee, K., Held, H., Kannen, A., Möllmann, C., Probst, W., Rambo, H., Cormier, R., & Stelzenmüller, V. (2020). Socio-ecological vulnerability to tipping points: A review of empirical approaches and their use for marine management. Science of the Total Environment, 705, 135838. https://doi.org/10.1016/j.scitotenv.2019.135838.

Lazzari, N., Becerro, M. A., & Martín-López, B. (2021). Assessing social-ecological vulnerability of coastal systems to fishing and tourism. Science of the Total Environment, 784, 147078. https://doi.org/10.1016/j.scitotenv.2021.147078.

Lebbe, Mohamed Farook Kalendher and Lokuge, Weena and Setunge, Sujeeva, and Zhang, Kevin (2014) Failure mechanisms of bridge infrastructure in an extreme flood event. In: Proceedings of the *1st International Conference on Infrastructure Failures and Consequences*, 16-20 July 2014, Melbourne, pp124-132. ISBN: 978-0-9925570-1-0.

Leta, B. M., & Adugna, D. (2023). Characterizing the level of urban Flood vulnerability using the social-ecological-technological systems framework, the case of Adama city, Ethiopia. Heliyon, 9(10), e20723. https://doi.org/10.1016/j.heliyon.2023.e20723.

Li, Z., Duque, F. Q., Grout, T., Bates, B., & Demir, I. (2023a). Comparative analysis of performance and mechanisms of flood inundation map generation using Height Above Nearest Drainage. *Environmental Modelling & Software*, *159*, 105565.

Li, Z., Xiang, Z., Demiray, B. Z., Sit, M., & Demir, I. (2023b). MA-SARNet: A one-shot nowcasting framework for SAR image prediction with physical driving forces. *ISPRS journal of photogrammetry and remote sensing*, 205, 176-190.

McPhearson, T., Cook, E. M., Berbés-Blázquez, M., Cheng, C. J., Grimm, N. B., Andersson, E., Barbosa, O., Chandler, D. G., Chang, H., Chester, M., Childers, D. L., Elser, S. R., Frantzeskaki, N., Grabowski, Z. R., Groffman, P. M., Hale, R. L., Iwaniec, D. M., Kabisch, N., Kennedy, C., . . . Troxler, T. G. (2022). A social-ecological-technological systems framework for urban ecosystem services. One Earth, 5(5), 505–518. https://doi.org/10.1016/j.oneear.2022.04.007.

Nasiri, H., Mohd Yusof, M. J., & Mohammad Ali, T. A. (2016). An overview to flood vulnerability assessment methods. Sustainable Water Resources Management, 2(3), 331–336. https://doi.org/10.1007/s40899-016-0051-x.

National Centers for Environmental Information (NCEI). (2020, December 29). Normalized Difference Vegetation Index CDR. Retrieved from https://www.ncei.noaa.gov/products/climate-data-records/normalized-difference-vegetation-index.

National Weather Service (2018). June 30, 2018, Central Iowa major flash flood event: National Oceanic and Atmospheric Administration web page, at https://www.weather.gov/dmx/20180630_EpicFlashFlood.

Nguyen, T. L., Tran, T. A., & Nguyen, H. N. (2023). An Overview of Indicator-Based Approach of flood Vulnerability Assessment. In New frontiers in regional science: Asian perspectives (pp. 187–204). https://doi.org/10.1007/978-981-99-5667-8_9.

NLCD 2019 Percent Developed Imperviousness (CONUS) | Multi-Resolution Land Characteristics (MRLC) Retrieved from https://www.mrlc.gov/data/nlcd-2019-percent-developed-imperviousness-conus.

Noori, S., Mohammadi, A., Ferreira, T. M., Ghaffari Gilandeh, A., & Mirahmadzadeh Ardabili, S. J. (2023). Modelling and mapping urban vulnerability index against potential structural fire-related risks: An integrated GIS–MCDM approach. Fire, 6(3), 107. https://doi.org/10.3390/fire6030107.

OpenStreetMap contributors. (2015) Planet dump [Data file from $date of database dump$]. Retrieved from https://planet.openstreetmap.org.

O'Shea, P. S., Vegrzyn, J. C., & Barnes, K. K. (2021). Flood of June 30–July 1, 2018, in the Fourmile Creek Basin, near Ankeny, Iowa. Open-file Report /. https://doi.org/10.3133/ofr20211044.

Pallathadka, A., Sauer, J., Chang, H., & Grimm, N. B. (2022). Urban flood risk and green infrastructure: Who is exposed to risk and who benefits from investment? A case study of three US Cities. Landscape and Urban Planning, 223. https://doi.org/10.1016/j.landurbplan.2022.104417.

Retchless, D., Frey, N., Wang, C., Hung, L. S., & Yarnal, B. (2014). Climate extremes in the United States: recent research by physical geographers. Physical Geography, 35(1), 3–21. https://doi.org/10.1080/02723646.2013.871191.

Rives, F., Antona, M., & Aubert, S. (2012). Social-ecological Functions and Vulnerability Framework to analyze forest policy reforms. Ecology and Society, 17(4). https://doi.org/10.5751/es-05182-170421.

Sadler, J. M., Haselden, N., Mellon, K., Hackel, A., Son, V., Mayfield, J., ... & Goodall, J. L. (2017). Impact of sea-level rise on roadway flooding in the Hampton Roads region, Virginia. Journal of Infrastructure Systems, 23(4), 05017006. doi.org/10.1061/(ASCE)IS.1943-555X.0000397.

Saharia, M., Kirstetter, P., Vergara, H., Gourley, J. J., & Hong, Y. (2017). Characterization of floods in the United States. Journal of Hydrology, 548, 524–535. https://doi.org/10.1016/j.jhydrol.2017.03.010.

Sauer, J., Pallathadka, A., Ajibade, I., Berbés-Blázquez, M., Chang, H., Cook, E. M., Grimm N.B., Iwaniec D.M., Lloyd R. & Post, G. C. (2023). Relating social, ecological, and technological vulnerability to future flood exposure at two spatial scales in four US cities. Sustainable Cities and Society, 99, 104880. https://doi.org/10.1016/j.scs.2023.104880.

Sermet, Y., Villanueva, P., Sit, M. A., & Demir, I. (2020). Crowdsourced approaches for stage measurements at ungauged locations using smartphones. *Hydrological Sciences Journal*, *65*(5), 813-822.

U.S. Census Bureau. (2022) "SEX BY AGE." American Community Survey, ACS 5-Year Estimates Detailed Tables, Table B01001, 2022. U.S. Department of Commerce. Retrieved January 16, 2024, from https://data.census.gov/.

U.S. Census Bureau. (2022) "Tenure." American Community Survey, ACS 5-Year Estimates Detailed Tables, Table B25003, 2022. U.S. Department of Commerce. Retrieved January 16, 2024, from https://data.census.gov/.

U.S. Census Bureau. (2022). "Median Household Income in the Past 12 Months (in 2022 Inflation-Adjusted Dollars)." American Community Survey, ACS 5-Year Estimates Detailed Tables, Table B19013, 2022. U.S. Department of Commerce. Retrieved January 16, 2024, from https://data.census.gov/.

U.S. Census Bureau. (2022). Demographic and Housing Estimates. American Community Survey, ACS 5-Year Estimates Data Profiles, Table DP05, 2022. U.S. Department of Commerce. Retrieved January 16, 2024, from https://data.census.gov/.

U.S. Energy Information Administration (EIA) (2024). Power Plants. Arcgis.com. Retrieved from https://eia.maps.arcgis.com/home/item.html?id=bf5c5110b1b944d299bb683cdbd02d2a#overview.

U.S. Fish & Wildlife Service (2023). “Download Seamless Wetlands Data by State | U.S. Fish & Wildlife Service.” Retrieved from https://www.fws.gov/program/national-wetlands-inventory/download-state-wetlands-data.

US Department of Commerce, N. (2015, August 10). Flood and flash flood definitions. National Weather Service. https://www.weather.gov.

US Environmental Protection Agency (EPA) (2013). “Toxics Release Inventory (TRI) Program | US EPA.” US EPA, 31 Jan. 2013, www.epa.gov/toxics-release-inventory-tri-program.

USGS. (2010). Floods of May 30 to June 15, 2008, in the Iowa River and Cedar River Basins, Eastern Iowa. Retrieved from https://pubs.usgs.gov.

USGS. (2025). National Structures Dataset (NSD) Iowa Shapefile - ScienceBase-Catalog. Www.sciencebase.gov. Retrieved from https://www.sciencebase.gov/.

Verma, P., Singh, R., Bryant, C., & Raghubanshi, A. S. (2020). Green space indicators in a social-ecological system: A case study of Varanasi, India. Sustainable Cities and Society, 60, 102261. https://doi.org/10.1016/j.scs.2020.102261

Xu, H., Demir, I., Koylu, C., & Muste, M. (2019). A web-based geovisual analytics platform for identifying potential contributors to culvert sedimentation. *Science of the Total Environment*, *692*, 806-817.

Zhou, Q., Leng, G., & Peng, J. (2018). Recent changes in the occurrences and damages of floods and droughts in the United States. Water, 10(9), 1109. https://doi.org/10.3390/w10091109

Zogg, J. (2014). The Top Five Iowa Floods. National Weather Service WFO: Des Moines, IA, USA.